Contribution of two-particle–two-hole final states to the nuclear response

Omar Benhar,[1,2] Alessandro Lovato,[3,4] and Noemi Rocco[1]

[1]*INFN and Department of Physics, "Sapienza" University, I-00185 Roma, Italy*
[2]*Center for Neutrino Physics, Virginia Tech, Blacksburg, Virginia 24061, USA*
[3]*Argonne Leadership Computing Facility, Argonne National Laboratory, Argonne, Illinois 60439, USA*
[4]*Physics Division, Argonne National Laboratory, Argonne, Illinois 60439, USA*

The excitation of two-particle–two-hole final states in neutrino-nucleus scattering has been advocated by many authors as the source of the excess cross section observed by the MiniBooNE Collaboration in the quasielastic sector. We analyze the mechanisms leading to the appearance of these final states and illustrate their significance through the results of accurate calculations of the nuclear electromagnetic response in the transverse channel. A novel approach, allowing for a consistent treatment of the amplitudes involving one- and two-nucleon currents in the kinematical region in which the nonrelativistic approximation breaks down, is outlined, and its preliminary results are reported.

I. INTRODUCTION

Experimental studies of neutrino-nucleus interactions carried out over the past decade [1–4] have provided ample evidence of the inadequacy of the relativistic Fermi gas model (RFGM), routinely employed in event generators, to account for both the complexity of nuclear dynamics and the variety of reaction mechanisms—other than single-nucleon knockout—contributing to the observed cross section.

A striking manifestation of the above problem is the large discrepancy between the predictions of Monte Carlo simulations and the double differential charged-current (CC) quasielastic (QE) cross section measured by the MiniBooNE Collaboration using a carbon target [4].

As pointed out by the authors of Ref. [5], improving the treatment of nuclear effects, which turns out to be one of the main sources of systematic uncertainty in the oscillation analysis [6], will require the development of a *comprehensive* and *consistent* description of neutrino-nucleus interactions, *validated* through extensive comparison to the large body of electron-nucleus scattering data [7,8].

The main difficulty involved in the generalization of the approaches successfully employed to study electron scattering to the case of neutrino interactions stems from the fact that, while the energy of the electron beam is fixed, in neutrino scattering the measured cross section results from the average over different beam energies, broadly distributed according to a flux Φ. Therefore, a measurement of the energy of the outgoing charged lepton in a CC QE interaction *does not* specify the energy transfer to the nuclear target, which largely determines the reaction mechanism. As shown in Refs. [9,10], the MiniBooNE double differential cross section corresponding to a specific muon energy bin turns out to receive comparable contributions from different mechanisms, which must be all taken into account in a consistent fashion.

Many authors have suggested that the excess CC QE cross section observed by the MiniBooNE collaboration is to be ascribed to the occurrence of events with two-particle–two-hole final states, not taken into account by the RFGM employed for data analysis [5,11,12]. The description of these

processes within a realistic model of nuclear dynamics requires that all mechanisms leading to their occurrence—initial-state correlations (ISC) among nucleons in the target nucleus, final-state correlations (FSC) between the struck nucleon and the spectator particles, and interactions involving two-nucleon meson-exchange currents (MEC)—be included. Within the independent particle model (IPM) of the nucleus, however, correlations are not taken into account, and two-particle–two-hole final states can only be excited through the action of two-body operators, such as those involved in the definition of MEC.

In this paper, we analyze the mechanisms leading to the appearance of two-particle–two-hole final states in the response of interacting many-body systems and argue that the interference between amplitudes involving one- and two-nucleon currents plays an important role. This feature clearly emerges from the results of a calculation of the transverse electromagnetic response of ^{4}He and of the corresponding sum rule of ^{12}C, evaluated using state-of-the-art models of the nuclear Hamiltonian and currents, within the Green's function Monte Carlo (GFMC) computational scheme [13].

In view of the extension of our study to the kinematical regime in which the nonrelativistic approximation is no longer applicable, we also outline a novel approach, based on a generalization of the factorization ansatz, underlying the spectral function formalism. This scheme, allowing for a consistent treatment of one- and two-nucleon current contributions, appears to be quite promising for applications to neutrino scattering.

The structure of the nuclear cross section, as well as its expression in terms of longitudinal and transverse structure functions, are reviewed in Sec. II, while Sec. III describes the theoretical approaches, based on nuclear many-body theory, developed to study electron-nucleus scattering. In Sec. III A we discuss the nonrelativistic regime and the results of GFMC calculations, while in Secs. III B and III C we derive the explicit expression of the two-particle–two-hole contribution to the cross section obtained from our approach and discuss the preliminary results of its application. Finally, in Sec. IV we summarize our findings and state the conclusions.

II. NUCLEAR CROSS SECTION AND RESPONSE FUNCTIONS

In the one-photon-exchange approximation, the double differential electron-nucleus cross section can be written in the form

$$\frac{d^2\sigma}{dE_{e'}d\Omega_{e'}} = \frac{\alpha^2}{q^4}\frac{E_{e'}}{E_e}L_{\mu\nu}W_A^{\mu\nu}, \quad (1)$$

where $k_e = (E_e, \mathbf{k}_e)$ and $k_{e'} = (E_{e'}, \mathbf{k}_{e'})$ are the four-momenta of the incoming and outgoing electrons, respectively, $\alpha = 1/137$ is the fine structure constant, $d\Omega_{e'}$ is the differential solid angle in the direction specified by $\mathbf{k}_{e'}$, and $q = k_e - k_{e'} = (\omega, \mathbf{q})$ is the four-momentum transfer.

The lepton tensor $L_{\mu\nu}$ is completely determined by lepton kinematics, while the nuclear response is described by the tensor $W_A^{\mu\nu}$, defined as

$$W_A^{\mu\nu}(\mathbf{q}, \omega) = \sum_N \langle 0|J_A^\mu|N\rangle\langle N|J_A^\nu|0\rangle\delta^{(4)}(P_0 + q - P_N), \quad (2)$$

where $|0\rangle$ and $|N\rangle$ denote the initial and final hadronic states, the four-momenta of which are $P_0 \equiv (E_0, \mathbf{p}_0)$ and $P_N \equiv (E_N, \mathbf{p}_N)$. The nuclear current can be written as a sum of one- and two-nucleon contributions, according to (see, e.g., Ref. [14])

$$J_A^\mu = \sum_i j_i^\mu + \sum_{j>i} j_{ij}^\mu. \quad (3)$$

The current j_i^μ describes interactions involving a single nucleon. In the QE sector, it can be expressed in terms of the measured vector form factors [15]. The two-nucleon contribution j_{ij}^μ, however, accounts for processes in which the beam particle couples to the currents arising from meson exchange between two interacting nucleons.

Equation (1) can be rewritten in terms of two response functions, denoted $R_L(\mathbf{q}, \omega)$ and $R_T(\mathbf{q}, \omega)$, describing interactions with longitudinally (L) and transversely (T) polarized photons, respectively. The resulting expression reads

$$\frac{d^2\sigma}{dE_e'd\Omega_e} = \left(\frac{d\sigma}{d\Omega_e}\right)_M[A_L(|\mathbf{q}|, \omega, \theta_e)R_L(|\mathbf{q}|, \omega) + A_T(|\mathbf{q}|, \omega, \theta_e)R_T(|\mathbf{q}|, \omega)], \quad (4)$$

where

$$A_L = \left(\frac{q^2}{\mathbf{q}^2}\right)^2, \quad A_T = -\frac{1}{2}\frac{q^2}{\mathbf{q}^2} + \tan^2\frac{\theta_e}{2}, \quad (5)$$

and $(d\sigma/d\Omega_e)_M = [\alpha\cos(\theta_e/2)/4E_e\sin^2(\theta_e/2)]^2$ is the Mott cross section.

The L and T structure functions can be readily expressed in terms of the components of the response tensor of Eq. (2). Choosing the z axis along the direction of the momentum transfer one finds

$$R_L = W_A^{00}, \quad (6)$$

$$R_T = \sum_{ij=1}^3\left(\delta_{ij} - \frac{q_iq_j}{\mathbf{q}^2}\right)W_A^{ij} = W_A^{xx} + W_A^{yy}. \quad (7)$$

Note that the above expressions are completely general and describe processes involving both one- and two-nucleon current operators.

It follows from Eqs. (1) and (2) that the nuclear cross section and response functions can be written as a sum of contributions corresponding to different hadronic final states $|N\rangle$. Consider, for example, the case of QE scattering, in which the final-state particles are nucleons only. For a carbon target we find

$$|N\rangle = |^{11}B, p\rangle, |^{11}C, n\rangle, |^{10}B, pn\rangle, |^{10}Be, pp\rangle, \ldots, \quad (8)$$

where the residual nucleus can be in any *bound* state.

The states $|N\rangle$ are usually classified according to the number of nucleons excited to the continuum and referred to as one-particle–one-hole (1p1h), two-particle–two-hole (2p2h), etc. In Eq. (8), $|^{11}B, p\rangle$ and $|^{11}C, n\rangle$ are 1p1h states, while $|^{10}B, pn\rangle$ and $|^{10}Be, pp\rangle$ are 2p2h states.

Neglecting the contributions of final states involving more than two nucleons in the continuum, the cross section can be written as

$$d\sigma = d\sigma_{1p1h} + d\sigma_{2p2h} \propto L_{\mu\nu}(W_{1p1h}^{\mu\nu} + W_{2p2h}^{\mu\nu}). \quad (9)$$

We recall that, in scattering processes involving *interacting* many-body systems, 2p2h final states can be produced through the action of *both* one- and two-nucleon currents.[1] However, for the matrix element of a one-body operator between the target ground state and a 2p2h final state to be nonvanishing, the effects of dynamical nucleon-nucleon (NN) correlations must be included in the description of the nuclear wave functions.

Correlations give rise to virtual scattering between nucleons in the target nucleus, leading to the excitation of the participating particles to continuum states. The ISC contribution to the 2p2h amplitude arises from processes in which the beam particle couples to *one* of these high-momentum nucleons. The FSC contribution, however, originates from scattering processes involving the struck nucleon and one of the spectator particles, which also result in the appearance of 2p2h final states.

III. MANY-BODY THEORY OF THE NUCLEAR RESPONSE

As discussed in the previous section, the calculation of the nuclear response requires the evaluation of the transition amplitudes $\langle 0|J_A^\mu|N\rangle$, involving both one- and two-nucleon current operators, as well as all possible final states. The initial state can be accurately described within the framework of nonrelativistic many-body theory using realistic models of the nuclear Hamiltonian, strongly constrained by nucleon-nucleon scattering data and nuclear phenomenology. The final state and the current operator, however, depend on momentum transfer, and their calculation in the kinematical region in which the non relativistic picture breaks down necessarily implies additional assumptions.

---

[1]It should be kept in mind that 1p1h final states can also be excited by both one- and two-nucleon currents.

A. Nonrelativistic regime

The approach based on the GFMC computational scheme provides a suitable framework to carry out accurate calculations of a variety of nuclear properties in the nonrelativistic regime, typically corresponding to $|\mathbf{q}| \lesssim 500$ MeV (for a recent review of quantum Monte Carlo methods for nuclear physics, see, e.g., Ref. [16]).

Valuable information on the L and T responses can be obtained from their Laplace transforms, also referred to as Euclidean responses, defined as

$$\widetilde{E}_{T,L}(\mathbf{q},\tau) = \int_{\omega_{\rm el}}^{\infty} d\omega e^{-\omega\tau} R_{T,L}(\mathbf{q},\omega). \tag{10}$$

The lower integration limit $\omega_{\rm el} = \mathbf{q}^2/2M_A$, M_A being the mass of the target nucleus, is the threshold of elastic scattering—corresponding to the $|N\rangle = |0\rangle$ term in the sum of Eq. (2)—the contribution of which is excluded.

Within GFMC, the Euclidean responses are evaluated from

$$\widetilde{E}_L(\mathbf{q},\tau) = \langle 0|\rho^*(\mathbf{q})e^{-(H-E_0)\tau}\rho(\mathbf{q})|0\rangle - |\langle 0|\rho(\mathbf{q})|0\rangle|^2 e^{-\omega_{\rm el}\tau}, \tag{11}$$

and

$$\widetilde{E}_T(\mathbf{q},\tau) = \langle 0|\mathbf{j}_T^{\dagger}(\mathbf{q})e^{-(H-E_0)\tau}\mathbf{j}_T(\mathbf{q})|0\rangle - |\langle 0|\mathbf{j}_T(\mathbf{q})|0\rangle|^2 e^{-\omega_{\rm el}\tau}, \tag{12}$$

where $\rho(\mathbf{q})$ and $\mathbf{j}_T(\mathbf{q})$ denote nonrelativistic reductions of the nuclear charge and transverse current operators, respectively [13].

Note that, although the states $|N\rangle \neq |0\rangle$ do not appear explicitly in Eqs. (11) and (12), the Euclidean responses include the effects of final-state interactions (FSI) of the particles involved in the electromagnetic interaction, both among themselves and with the spectator nucleons.

The Euclidean responses at $\tau = 0$ are directly related to the sum rules of the L and T responses, obtained from ω integration after removing the trivial energy and momentum dependence associated with the nucleon form factor [17]:

$$S_{T,L}(|\mathbf{q}|) = \frac{C_{T,L}}{\left[G_E^p\left(Q_{\rm QE}^2\right)\right]^2} \int_{\omega_{\rm el}}^{\infty} d\omega R_{T,L}(\mathbf{q},\omega). \tag{13}$$

In the above equation, $G_E^p(Q_{\rm QE}^2)$ is the electric proton form factor evaluated in QE kinematics, i.e., at $Q_{\rm QE}^2 = \mathbf{q}^2 - \omega_{\rm QE}^2$, with $\omega_{\rm QE} = (\sqrt{\mathbf{q}^2 + m^2} - m)$, where m is the proton mass. The coefficients appearing in Eq. (13) are defined as

$$C_L = \frac{1}{Z}, \quad C_T = \frac{2}{Z\mu_p^2 + N\mu_n^2} \frac{m^2}{\mathbf{q}^2}, \tag{14}$$

where Z is the proton charge, $N = A - Z$ is the number of neutrons and μ_p and μ_n are the proton and neutron magnetic moments, respectively.

The inversion of the Laplace transform, needed to retrieve the energy dependence of the responses, is long known to involve severe difficulties. A groundbreaking result has been recently reported by the authors of Ref. [18], who exploited the maximum entropy technique to obtain the L and T responses of ^{4}He.
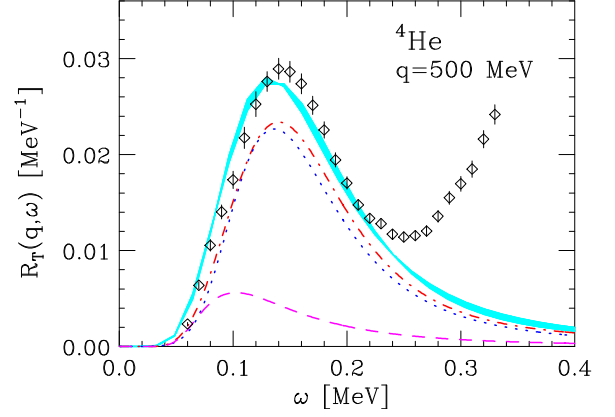

FIG. 1. (Color online) Transverse response function of ^{4}He, obtained within the approach of Ref. [18]. The shaded area shows the results of the full calculation, with the associated uncertainty arising from the inversion of the Euclidean response, while the dotted line has been obtained including the one-nucleon current only. The dot-dashed line represents the response computed neglecting the interference term, the contribution of which is displayed by the dashes. The data are taken from Ref. [13].

Figure 1 shows the breakdown of the transverse response of ^{4}He at $|\mathbf{q}| = 500$ MeV—computed within the approach of Ref. [18]—into one-nucleon current, two-nucleon current, and interference contributions. Note that the quantity displayed in the figure is normalized dividing by the squared proton form factor.

It clearly appears that including the two-nucleon currents leads to a sizable enhancement of the response and that the large positive contribution of the interference term peaks at energy loss $\omega < \omega_{\rm QE}$. This feature is a direct consequence of nucleon-nucleon correlations, neglected in the mean-field approach. The agreement between the GFMC results and the data of Ref. [13] turns out to be remarkably good.

The extension of the procedure employed to obtain the ^{4}He response to heavier nuclei, such as carbon, is still out of reach of the available computational capabilities. However, valuable information can be extracted from the analyses of the sum rules.

The results of numerical calculations of the carbon $S_T(|\mathbf{q}|)$, displayed in Fig. 2, clearly show that interference terms provide a sizable fraction of the sum rule. At momentum transfer $|\mathbf{q}| \gtrsim 300$ MeV, their contribution turns out to be comparable to—in fact even larger than—that obtained squaring the matrix element of the two-nucleon current.

B. Relativistic regime: The factorization ansatz

The results of Figs. 1 and 2 clearly point to the need for a consistent treatment of correlations and MEC, within a formalism suitable for application in the kinematical region in which the nonrelativistic approximation is known to fail. This section describes the derivation of the approach based on factorization of the nuclear matrix elements. For ease of presentation, we consider the response of uniform and
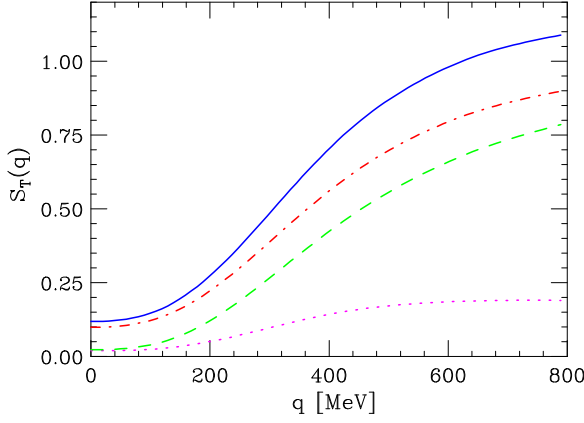
FIG. 2. (Color online) Sum rule of the electromagnetic response of carbon in the transverse channel. The dashed line shows the results obtained including the one-nucleon current only, while the solid line corresponds to the full calculation. The dot-dashed line represents the sum rule computed neglecting the interference term, the contribution of which is displayed by the dotted line. The results are normalized so that the dashed line approaches unity as $|\mathbf{q}| \to \infty$. Monte Carlo errors bars are not visible on the scale of the figure.

isospin-symmetric nuclear matter. However, the generalization to atomic nuclei does not involve any substantial problems.

The effects of ISC on the nuclear cross section at large momentum transfer can be taken into account using the spectral function formalism [19,20]. The conceptual framework underlying this approach is provided by the impulse approximation (IA), i.e., the assumption that at momentum transfer such that $|\mathbf{q}|^{-1} \ll d$, d being the average separation distance between nucleons in the target nucleus, the nuclear cross section reduces to the incoherent sum of cross sections describing scattering processes involving individual nucleons. As a consequence, the contribution of the two-nucleon current can be disregarded, and the final state $|N\rangle$ of Eq. (2) can be written in the factorized form

$$|N\rangle = |\mathbf{p}\rangle \otimes |n_{A-1}, \mathbf{p}_n\rangle. \tag{15}$$

In the above equation, $|\mathbf{p}\rangle$ is the state of a noninteracting nucleon carrying momentum $\mathbf{p}$, while $|n_{A-1}, \mathbf{p}_n\rangle$ describes the $(A-1)$-particle spectator system in the state n, with momentum $\mathbf{p}_n$. Note that, owing to NN correlations, $|n_{A-1}\rangle$ is not restricted to being a bound state [see Eq. (8)].

Within the IA, the contribution to the nuclear cross section arising from interactions involving the one-nucleon current can be written in terms of the cross sections of elementary scattering processes off individual nucleons, the momentum ($\mathbf{k}$) and removal energy (E) of which are distributed according to the spectral function $P(\mathbf{k}, E)$ [19], defined as

$$P(\mathbf{k}, E) = \sum_n |\langle n_{A-1}, \mathbf{p}_n | a_{\mathbf{k}} | 0 \rangle|^2 \delta(E + E_0 - E_n). \tag{16}$$

In the above equation, E_n is the energy of the $(A-1)$-nucleon state, and the operator $a_{\mathbf{k}}$ removes a nucleon of momentum $\mathbf{k}$ from the nuclear ground state.

The resulting expression of the cross section is [8]

$$d\sigma_{IA} = \sum_i \int d^3k\, dE\, P_i(\mathbf{k}, E) d\sigma_i. \tag{17}$$

Note that $P_i(\mathbf{k}, E)$ describes an intrinsic property of the target nucleus, independent of momentum transfer, and as such can be safely obtained from nonrelativistic many-body theory. However, the matrix elements of the nucleon current entering the definition of $d\sigma_i$ can be computed using its fully relativistic form.

Exploiting the Källén-Lehman representation of the two-point Green's function, the spectral function appearing in Eq. (17), can be conveniently split into two parts, displaying distinctly different energy dependencies [21]. The single-particle part $P_{1h}(\mathbf{k}, E)$, obtained from Eq. (16) including *bound* 1h states only, exhibits a pole at $E = -e_k$, e_k being the energy of a nucleon in the hole state of momentum $\mathbf{k}$. The continuum part, however, is smooth and extends to large values of energy and momentum. Its leading term, corresponding to 2h1p states of the residual $(A-1)$-particle system in which one nucleon is excited to a state outside the Fermi sea, can be written in the form

$$P_{2h1p}(\mathbf{k}, E) = \int d^3h\, d^3h'\, d^3p' |\Phi_k^{hh'p'}|^2 \theta(k_F - |\mathbf{h}|)$$
$$\times \theta(k_F - |\mathbf{h}'|)\theta(|\mathbf{p}'| - k_F)$$
$$\times \delta(E + e_h + e_{h'} - e_{p'}), \tag{18}$$

where the integration includes a sum over the indices associated with discrete degrees of freedom, and

$$\Phi_k^{hh'p'} = \langle 0|\{|\mathbf{k}\rangle \otimes |\mathbf{h}\mathbf{h}'\mathbf{p}'\rangle\}. \tag{19}$$

Note that momentum conservation requires that the expression of $\Phi_k^{hh'p'}$ involve a $\delta(\mathbf{h} + \mathbf{h}' - \mathbf{p}' - \mathbf{k})$.

As pointed out above, in the presence of ground-state correlations both parts of the spectral function provide nonvanishing contributions to the cross section of Eq. (17).

Figure 3 shows the 1p1h and 2p2h components of the electron-carbon cross section arising from ISC. The calculations have been performed at $E_e = 961$ MeV and $\theta_e = 37.5°$, using Eq. (17) with the spectral function of Ref. [20] and the parametrization of the nucleon form factors of Ref. [22]. The solid line corresponds to the results of the full calculation, while the dot-dashed and dashed lines have been obtained using the pole and continuum parts of the spectral function, which amounts to taking into account only 1p1h or 2p2h final states, respectively. The distinct energy dependence of the 2p2h contribution, providing ∼10% of the total QE cross section, is clearly visible.

The importance of relativistic effects can be gauged comparing the solid and dashed lines of Fig. 4, representing the carbon cross sections obtained from Eq. (17) using relativistic and nonrelativistic kinematics, respectively. It clearly appears that in a kinematical setup corresponding to $|\mathbf{q}| \sim 585$ MeV at $\omega = \omega_{QE}$ relativistic kinematics sizeably affects both position and width of the QE peak.

The factorization ansatz of Eq. (15) can be readily extended to allow for a consistent treatment of the amplitudes involving
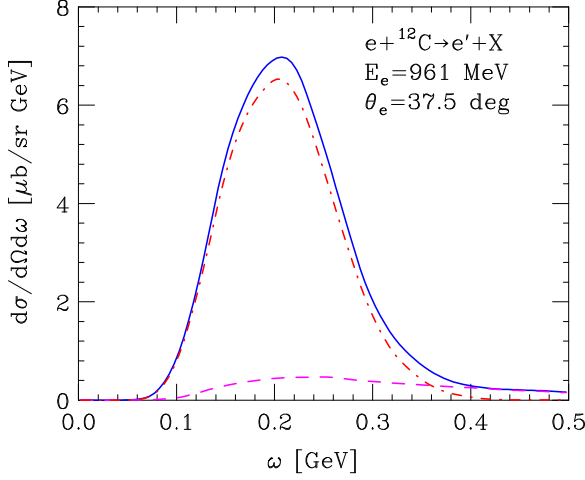
FIG. 3. (Color online) Cross section of the process $e + {}^{12}C \rightarrow e' + X$ at beam energy $E_e = 961$ MeV and electron scattering angle $\theta_e = 37.5°$, computed using Eq. (17) with the spectral function of Ref. [20]. The solid line shows the results of the full calculation, while the breakdown into 1p1h and 2p2h contributions is illustrated by the dot-dashed and dashed lines, respectively.

one- and two-nucleon currents. The resulting expression is

$$|N\rangle = |\mathbf{pp'}\rangle \otimes |m_{A-2}, \mathbf{p}_m\rangle, \qquad (20)$$

where the states $|\mathbf{pp'}\rangle$ and $|m_{A-2}, \mathbf{p}_m\rangle$ describe two noninteracting nucleons of momenta $\mathbf{p}$ and $\mathbf{p'}$ and the $(A-2)$-particle residual system, respectively.

Using Eq. (20), the nuclear matrix element of the two-nucleon current can be written in terms of two-body matrix elements according to

$$\langle N|j^\mu_{ij}|0\rangle = \int d^3k\, d^3k'\, M_m(\mathbf{k},\mathbf{k}')\langle \mathbf{pp'}|j^\mu_{ij}|\mathbf{kk'}\rangle, \qquad (21)$$
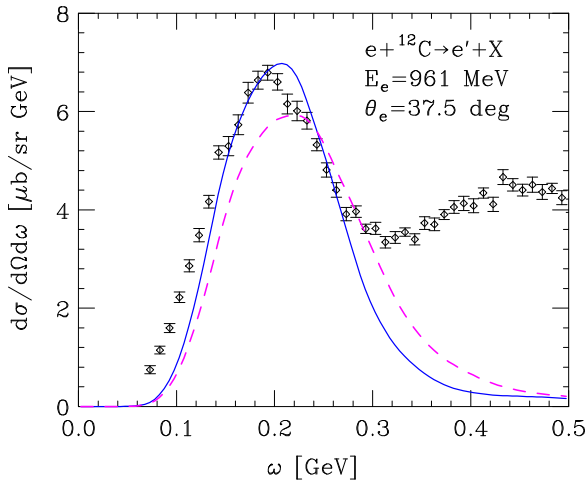

FIG. 4. (Color online) Electron-carbon cross section obtained from Eq. (17) using relativistic (solid line) and nonrelativistic (dashed line) kinematics. The experimental data are from Ref. [23].

with $M_m(\mathbf{k},\mathbf{k}')$ given by

$$M_m(\mathbf{k},\mathbf{k}') = \{\langle m_{(A-2)}, \mathbf{p}_m| \otimes \langle \mathbf{kk'}|\}|0\rangle. \qquad (22)$$

From the above equations it follows that the evaluation of the nuclear transition matrix element involving the two-nucleon current reduces to the calculations of the nuclear amplitude $M_m(\mathbf{k},\mathbf{k}')$ and of the matrix element of the current operator between free nucleon states. The former, being independent of momentum transfer, can be carried out using the nonrelativistic formalism, while the latter does not involve any approximations.

The connection with the spectral function formalism becomes apparent noting that the two-nucleon spectral function $P(\mathbf{k},\mathbf{k}',E)$, yielding the probability of removing *two nucleons* of momenta $\mathbf{k}$ and $\mathbf{k}'$ from the nuclear ground state leaving the residual system with excitation energy E, is defined as [compare to Eq. (16)] [24]

$$P(\mathbf{k},\mathbf{k}',E) = \sum_m |M_m(\mathbf{k},\mathbf{k}')|^2 \delta(E + E_0 - E_m), \qquad (23)$$

with $M_m(\mathbf{k},\mathbf{k}')$ given by Eq. (22).

The two-nucleon spectral function of uniform and isospin-symmetric nuclear matter at equilibrium density has been calculated by the authors of Ref. [24] using a realistic Hamiltonian. The resulting relative momentum distribution, defined as

$$n(\mathbf{Q}) = 4\pi |\mathbf{Q}|^2 \int d^3K\, n\left(\frac{\mathbf{K}}{2} + \mathbf{Q}, \frac{\mathbf{K}}{2} - \mathbf{Q}\right), \qquad (24)$$

where $\mathbf{K} = \mathbf{k} + \mathbf{k}'$, $\mathbf{Q} = (\mathbf{k} - \mathbf{k}')/2$, and

$$n(\mathbf{k},\mathbf{k}') = \int dE\, P(\mathbf{k},\mathbf{k}',E), \qquad (25)$$

is shown by the solid line of Fig. 5. Comparison with the prediction of the Fermi gas (FG) model, represented by the dashed line, indicates that correlations give rise to a sizable quenching of the peak of the distribution, along with the appearance of a high-momentum tail.
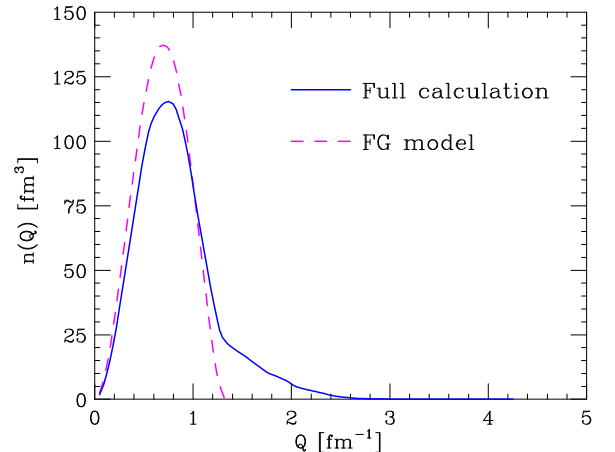

FIG. 5. (Color online) Relative momentum distribution of a nucleon pair in isospin-symmetric nuclear matter at equilibrium density.

C. 1p1h and 2p2h contributions to the transition matrix element

The extended factorization ansatz discussed in the previous section provides a scheme allowing for a clear-cut identification of the 1p1h and 2p2h contributions to the nuclear cross section in the presence of two-nucleon currents.

Let us consider the contribution of 2p2h final states to the response tensor of Eq. (2),

$$
\begin{aligned}
W^{\mu\nu}_{2p2h} = \int d^3h\, d^3h'\, d^3p\, d^3p'\, \theta(k_F - |\mathbf{h}|)\theta(k_F - |\mathbf{h}'|) \\
\times\, \theta(|\mathbf{p}| - k_F)\theta(|\mathbf{p}'| - k_F)\langle 0|J^\mu|\mathbf{hh'pp'}\rangle \\
\times\, \langle \mathbf{hh'pp'}|J^\nu|0\rangle\delta(\omega + E_0 - E_{hh'pp'}) \\
\times\, \delta(\mathbf{q} + \mathbf{h} + \mathbf{h'} - \mathbf{p} - \mathbf{p'}),
\end{aligned}
\tag{26}
$$

where $\mathbf{q}$ is the total momentum transfer, while $\mathbf{h},\mathbf{h}'$ and $\mathbf{p},\mathbf{p}'$ are the momenta of the hole and particle states, respectively. The structure of the current operator, involving one- and two-body terms, can be best understood from its momentum space expression,

$$
\begin{aligned}
J^\mu(\mathbf{k_1},\mathbf{k_2}) &= \int d^3x_1 d^3x_2\, J^\mu(\mathbf{x_1},\mathbf{x_2})\, e^{-i(\mathbf{k_1}\cdot\mathbf{x_1} + \mathbf{k_2}\cdot\mathbf{x_2})} \\
&= j^\mu_1(\mathbf{k_1})\delta(\mathbf{k_2}) + j^\mu_2(\mathbf{k_2})\delta(\mathbf{k_1}) + j^\mu_{12}(\mathbf{k_1},\mathbf{k_2}),
\end{aligned}
\tag{27}
$$

showing how the total momentum transfer, $\mathbf{q} = \mathbf{k_1} + \mathbf{k_2}$, is shared between the two nucleons involved in the electromagnetic interaction, labeled by the indices 1 and 2.

Within the factorization scheme, the matrix element of the one-nucleon current operator can be readily evaluated inserting a complete set of states describing a noninteracting nucleon. The resulting expression is

$$
\langle 0|j^\mu_1|\mathbf{hh'pp'}\rangle = \int d^3k\, \Phi_k^{hh'p'}\langle \mathbf{k}|j^\mu_1|\mathbf{p}\rangle,
\tag{28}
$$

with $\Phi_k^{hh'p'}$ defined by Eq. (19).

The calculation of the matrix element of the two-nucleon current exploits the fact that, in analogy with $P(\mathbf{k},E)$, the two-nucleon spectral function of Eq. (23) can be separated into two parts, characterized by their analytical structure. The component corresponding to *bound* 2h states of the $(A-2)$-nucleon system exhibits a pole located at $E = -(e_k + e_{k'})$, whereas the continuum states, the dominant of which is the 3h1p state, give rise to a smooth background.

It follows that, within the factorization scheme, the contribution to $W^{\mu\nu}_{2p2h}$ arising from amplitudes involving *only* the two-nucleon current is obtained from the 2h component of $P(\mathbf{k},\mathbf{k}',E)$, which can be written in the form [24]

$$
\begin{aligned}
P_{2h}(\mathbf{k},\mathbf{k}',E) = \int d^3h\, d^3h'\, |\Phi_{kk'}^{hh'}|^2 \delta(E + e_h + e_{h'}), \\
\times\, \theta(k_F - |\mathbf{h}|)\theta(k_F - |\mathbf{h}'|).
\end{aligned}
\tag{29}
$$

In the above equation, $\Phi_{kk'}^{hh'}$ is related to the overlap between the target ground state and the 2h state of the $(A-2)$-nucleon system through

$$
\Phi_{kk'}^{hh'} = \langle 0|\{|\mathbf{kk'}\rangle \otimes |\mathbf{hh'}\rangle\}.
\tag{30}
$$

The diagrammatic analysis of the cluster expansion of $\Phi_{kk'}^{hh'}$ in uniform and isospin-symmetric nuclear matter, carried out by

the authors of Ref. [24], shows that only unlinked graphs (i.e., graphs in which the points reached by the $\mathbf{k}$, $\mathbf{k}'$ lines are not connected to one other by any dynamical or statistical correlation lines) survive in the $A \to \infty$ limit, the contributions of linked diagrams being of order $1/A$. It follows that

$$
\Phi_{kk'}^{hh'} = \phi_k^h \phi_{k'}^{h'} \delta(\mathbf{h} - \mathbf{k})\delta(\mathbf{h}' - \mathbf{k}'),
\tag{31}
$$

where ϕ_k^h is the the Fourier transform of the overlap between the ground state and the $1h$ $(A-1)$-nucleon state, the calculation of which is discussed in Ref. [19].

Collecting the above results, we can write the expression of the response tensor obtained from the extended factorization ansatz as a sum of three contributions. The terms involving the squared amplitudes of the matrix elements involving one- and two-nucleon currents can be written in terms of the appropriate contributions to the one- and two-nucleon spectral functions, according to

$$
\begin{aligned}
W^{\mu\nu}_{2p2h,11} = \int d^3k \int dE\, P_{2h1p}(\mathbf{k},E)\langle \mathbf{k}|j^\mu_1|\mathbf{k+q}\rangle \\
\times\, \langle \mathbf{k+q}|j^\nu_1|\mathbf{k}\rangle\delta(\omega - E - e_{|k+q|})\theta(|\mathbf{k+q}| - k_F)
\end{aligned}
\tag{32}
$$

and

$$
\begin{aligned}
W^{\mu\nu}_{2p2h,22} = \int d^3k\, d^3k'\, d^3p\, d^3p' \int dE\, P_{2h}(\mathbf{k},\mathbf{k}',E) \\
\times\, \langle \mathbf{kk'}|j^\mu_{12}|\mathbf{pp'}\rangle\langle \mathbf{pp'}|j^\nu_{12}|\mathbf{kk'}\rangle \\
\times\, \delta(\mathbf{k} + \mathbf{k'} + \mathbf{q} - \mathbf{p} - \mathbf{p'})\delta(\omega - E - e_p - e_{p'}) \\
\times\, \theta(|\mathbf{p}| - k_F)\theta(|\mathbf{p}'| - k_F).
\end{aligned}
\tag{33}
$$

The interference term, however, involves a product of the nuclear amplitudes entering the definition of the spectral functions. The resulting expression is

$$
\begin{aligned}
W^{\mu\nu}_{2p2h,12} = \int d^3k\, d^3\xi\, d^3\xi'\, d^3h\, d^3h'\, d^3p\, d^3p'\, \phi_\xi^{h*} \phi_{\xi'}^{h'*} \delta(\mathbf{h} - \boldsymbol{\xi}) \\
\times\, \delta(\mathbf{h}' - \boldsymbol{\xi}')\big[\Phi_k^{hh'p'}\langle \mathbf{k}|j^\mu_1|\mathbf{p}\rangle + \Phi_k^{hh'p}\langle \mathbf{k}|j^\mu_2|\mathbf{p}'\rangle\big] \\
\times\, \langle \mathbf{p},\mathbf{p}'|j^\nu_{12}|\boldsymbol{\xi},\boldsymbol{\xi}'\rangle\, \delta(\mathbf{h} + \mathbf{h'} + \mathbf{q} - \mathbf{p} - \mathbf{p'}) \\
\times\, \delta(\omega + e_h + e_{h'} - e_p - e_{p'})\theta(|\mathbf{p}| - k_F) \\
\times\, \theta(|\mathbf{p}'| - k_F) + \text{H.c.}
\end{aligned}
\tag{34}
$$

Extensive numerical calculations of the electron-carbon cross section based on the formalism described in this paper are under way. However, they involve a number of nontrivial novel developments, e.g., the derivation of the two-hole contributions to the nuclear spectral function, the discussion of which will require a separate presentation.

Figure 6 shows the transverse electromagnetic response of carbon at $|\mathbf{q}| = 570$ MeV computed using the carbon spectral function of Ref. [20] and approximating the two-hole spectral function of carbon with that of uniform nuclear matter, at density corresponding to Fermi momentum $k_F = 221$ MeV. Note that this is *not* the same as working within the FG model. We use overlaps—the functions ϕ_k^h defined by Eqs. (30) and (31)—obtained from the *ab initio* approach of Refs. [19,21,24], based on a realistic nuclear Hamiltonian including two- and three-nucleon interactions.
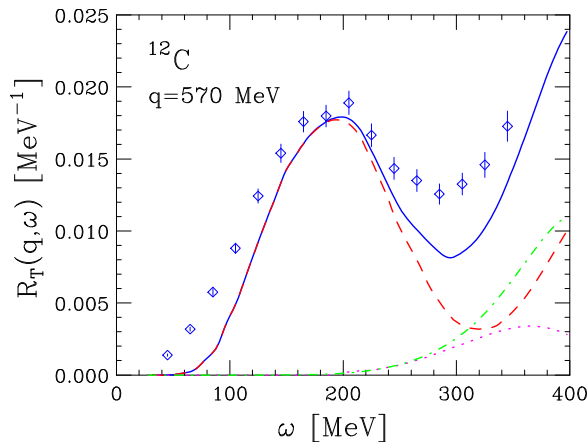
FIG. 6. (Color online) Electromagnetic response of carbon in the transverse channel, at momentum transfer $|\mathbf{q}| = 570$ MeV. The solid line represents the results of the full calculation, whereas the dashed line has been obtained including only amplitudes involving the one-body current. The contributions arising from the two-nucleon current are illustrated by the dot-dashed and dotted lines, corresponding to the pure two-body current transition probability and the interference term, respectively. The experimental data are taken from Ref. [28].

Owing to short-range correlations, which move strength from the 1p1h to the 2p2h sector, the resulting occupation of the momentum eigenstates is reduced by ~20%.

Interaction effects also affect the initial-state energies of the knocked-out nucleons [19,20], thus shifting the threshold of the two-nucleon current contributions with respect to the predictions of the FG model [25,26].

It has to be pointed out that the correlation contribution to the carbon spectral function of Ref. [20] is obtained from nuclear-matter results. Therefore, the use of nuclear matter overlaps in the matrix elements of the two-nucleon current entering the interference terms appears to be consistent.

We have used the fully relativistic expression of the two-nucleon current described in Refs. [25,26], with the same form factors and Δ width.

The solid line of Fig. 6 represents the results of the full calculation, whereas the dashed line has been obtained including only the amplitudes involving the one-body current. The contributions arising from the two-nucleon current are illustrated by the dash-dotted and dotted lines, corresponding to the pure two-body current transition probability and the interference term, respectively. The latter turns out to be sizable, its contribution being comparable to the total two-body current response for $\omega \lesssim 350$ MeV. Although our results still need to be improved and do not include the corrections taking into account the effects of FSI, in Fig. 6 we have also included, for comparison, the data resulting from the analysis of Ref. [28].

IV. CONCLUSIONS

We have analyzed the mechanisms—correlations in the initial and final states and coupling to MEC—leading to the excitation of 2p2h final states in the nuclear response to

electromagnetic interactions. In the nonrelativistic regime, in which highly accurate calculations consistently taking into account all these mechanisms are feasible, our results confirm the findings of Ref. [13].

In the transverse channel, the contribution of processes involving the two-nucleon current is sizable and extends well into the kinematical region corresponding to energy transfer $\omega \sim \omega_{\mathrm{QE}}$, in which single-nucleon knockout is dominant.

The important role played by interference between the amplitudes involving one- and two-body currents clearly implies that correlation effects must be included in any model aimed at describing the nuclear cross section in the 2p2h sector. This point was clearly stated, over three decades ago, in the pioneering work of Ref. [27], the authors of which also remarked on the inadequacy of the treatment of correlations based on lowest-order perturbative pion exchange. However, combining a realistic and consistent description of correlations and MEC in the kinematical region in which the nonrelativistic approximation is no longer applicable involves serious difficulties.

To overcome this problem, we have developed a novel approach based on the factorization ansatz underlying the spectral function formalism, widely and successfully employed to describe the nuclear response in the 1p1h sector. The preliminary results obtained within this approach, shown in Fig. 6, provide a fairly good description of the measured transverse response of carbon at $|\mathbf{q}| = 570$ MeV.

A comparison between the results of Fig. 6 and the GFMC results of Fig. 1 shows distinctive discrepancies in both magnitude and energy dependence of the two-body current contributions. While part of the disagreement is likely to originate from differences in the two-nucleon currents employed in Ref. [18], as well as from the nonrelativistic nature of the GFMC calculations, the large interference contribution in the region of the QE peak observed in Fig. 1 may arise from interference between amplitudes involving the one- and two-body currents and 1p1h final states. A careful analysis of these terms, which were found to be sizable in the pioneering work of Ref. [29], is being carried out, and will be discussed elsewhere.

The main assumption implied in the factorization of the 2p2h final states is the treatment of the knocked-out nucleons as free particles, which amounts to neglecting their interactions, both among themselves and with the spectator nucleons. Antisymmetrization under exchange between any of the outgoing particles and the spectators is also disregarded.

The factorized nuclear transition amplitudes involving the one-nucleon current can be corrected—to include the effects of final-state interactions in the QE sector—using an extension of the spectral function formalism, as discussed in Ref. [30]. The resulting modifications lead to (i) a shift in energy transfer of the differential cross section, arising from interactions between the knocked-out nucleon and the mean field of the recoiling nucleus and (ii) a redistribution of the strength from the quasifree peak to the tails, resulting from rescattering processes. Theoretical studies of electron-nucleus scattering suggest that in the kinematical region relevant to the MiniBooNE analysis the former mechanism—which does

not involve the appearance of 2p2h final states—provides the dominant contribution and can be taken into account through an optical potential [31].

The corrections to the factorized amplitudes involving the two-nucleon current also include interactions between the two knocked-out particles. A careful analysis of these processes is certainly needed. However, the results of Shen *et al.*, who carried out an accurate calculation of the neutrino-deuteron cross section over a broad kinematical range, suggest that their effect becomes negligibly small at beam energies larger than ~500 MeV [32].

In conclusion, we believe that the approach described in this paper provide a viable and promising scheme for the development of a unified treatment of processes involving one- and two-nucleon currents, applicable in the kinematical region relevant to accelerator-based neutrino oscillation searches.

Therefore, it may, in fact, be regarded as a step towards the *new paradigm* advocated by the authors of Refs. [5,9].

[1] R. Gran *et al.* (K2K Collaboration), Phys. Rev. D **74**, 052002 (2006).

[2] A. A. Aguilar Arevalo *et al.* (MiniBooNE Collaboration), Phys. Rev. Lett. **100**, 032301 (2008).

[3] V. Lyubushkin *et al.* (NOMAD Collaboration), Eur. Phys. J. C **63**, 355 (2009).

[4] A. A. Aguilar-Arevalo *et al.* (MiniBooNE Collaboration), Phys. Rev. D **81**, 092005 (2010).

[5] O. Benhar, P. Coletti, and D. Meloni, Phys. Rev. Lett. **105**, 132301 (2010).

[6] K. Abe *et al.* (T2K Collaboration), Phys. Rev. D **88**, 032002 (2013).

[7] O. Benhar, N. Farina, H. Nakamura, M. Sakuda, and R. Seki, Phys. Rev. D **72**, 053005 (2005).

[8] O. Benhar, D. Day, and I. Sick, Rev. Mod. Phys. **80**, 189 (2008).

[9] O. Benhar, Nucl. Phys. B, Proc. Suppl. **229–232**, 174 (2012).

[10] O. Benhar, J. Phys. Conf. Ser. **408**, 012042 (2013).

[11] M. Martini, M. Ericson, G. Chanfray, and J. Marteau, Phys. Rev. C **80**, 065501 (2009); **81**, 045502 (2010).

[12] J. Nieves, I. Ruiz Simo, and M. J. Vicente Vacas, Phys. Lett. B **707**, 72 (2012).

[13] J. Carlson, J. Jourdan, R. Schiavilla, and I. Sick, Phys. Rev. C **65**, 024002 (2002).

[14] J. Carlson and R. Schiavilla, Rev. Mod. Phys. **70**, 743 (1998).

[15] C. F. Perdrisat, V. Punjabi, and M. Vanderhäghen, Prog. Part. Nucl. Phys. **59**, 694 (2007).

[16] J. Carlson, S. Gandolfi, F. Pederiva, Steven C. Pieper, R. Schiavilla, K. E. Schmidt, and R. B. Wiringa, arXiv:1412.3081v2 [nucl-th].

[17] A. Lovato, S. Gandolfi, R. Butler, J. Carlson, E. Lusk, S. C. Pieper, and R. Schiavilla, Phys. Rev. Lett. **111**, 092501 (2013).

[18] A. Lovato, S. Gandolfi, J. Carlson, Steven C. Pieper, and R. Schiavilla, Phys. Rev. C **91**, 062501(R) (2015).

[19] O. Benhar, A. Fabrocini, and S. Fantoni, Nucl. Phys. A **505**, 267 (1989).

[20] O. Benhar, A. Fabrocini, S. Fantoni, and I. Sick, Nucl. Phys. A **579**, 493 (1994).

[21] O. Benhar, A. Fabrocini, and S. Fantoni, Phys. Rev. C **41**, R24(R) (1990).

[22] R. Bradford, A. Bodek, H. Budd, and J. Arrington, Nucl. Phys. B, Proc. Suppl. **159**, 127 (2006).

[23] R. M. Sealock, K. L. Giovanetti, S. T. Thornton, Z. E. Meziani, O. A. Rondon-Aramayo, S. Auffret, J. P. Chen, D. G. Christian, D. B. Day, J. S. McCarthy, R. C. Minehart, L. C. Dennis, K. W. Kemper, B. A. Mecking, and J. Morgenstern, Phys. Rev. Lett. **62**, 1350 (1989).

[24] O. Benhar and A. Fabrocini, Phys. Rev. C **62**, 034304 (2000).

[25] M. J. Dekker, P. J. Brussaard, and J. A. Tjon, Phys. Rev. C **49**, 2650 (1994).

[26] A. De Pace, M. Nardi, W. A. Alberico, T. W. Donnelly, and A. Molinari, Nucl. Phys. A **726**, 303 (2003).

[27] W. M. Alberico, M. Ericson, and A. Molinari, Ann. Phys. **154**, 356 (1984).

[28] J. Jourdan, Nucl. Phys. A **603**, 117 (1996).

[29] A. Fabrocini, Phys. Rev. C **55**, 338 (1997).

[30] O. Benhar, Phys. Rev. C **87**, 024606 (2013).

[31] A. M. Ankowski, O. Benhar, and M. Sakuda, Phys. Rev. D **91**, 033005 (2015).

[32] G. Shen, L. E. Marcucci, J. Carlson, S. Gandolfi, and R. Schiavilla, Phys. Rev. C **86**, 035503 (2012).